Hydrodynamic Granulation of Oxygenic Photogranules

Journal:	*Environmental Science: Water Research & Technology*
Manuscript ID	EW-ART-10-2020-000957.R1
Article Type:	Paper

Water Impact Statement

Photogranular technology presents potential to treat wastewater without energy intensive aeration. It also shows an ability to recover potential chemical energy in wastewater by carbon fixation. The current study presents new methods to produce seed oxygenic photogranules, involving hydrodynamic batches of activated sludge. The study discusses why granulation of photogranules occurs in widely varying settings but still in limited environments.

Hydrodynamic Granulation of Oxygenic Photogranules

Joseph G. Gikonyo[‡], Abeera A. Ansari[‡], Ahmed S. Abouhend [‡], John E. Tobiason[‡], Chul Park[*‡,]

[‡]Department of Civil and Environmental Engineering, University of Massachusetts Amherst, MA 01003, USA.

[*]Corresponding author: chulp@umass.edu

ABSTRACT

Oxygenic photogranules (OPGs), granular assemblages of phototrophic and chemotrophic microbes, offer a promising biotechnology for wastewater treatment with self-aerating potential. Currently, the seed OPG is produced under hydrostatic conditions with activated-sludge inoculum. We investigated the development of OPGs under hydrodynamic conditions employing batches with different light, shear, and inoculum conditions. The results demonstrated hydrodynamic granulation of OPGs from activated sludge, presenting opportunities for rapid (less than 8 days) and bulk development. From the matrix of conditions investigated, we found that granulation occurs only with some combinations of different magnitudes of these input energies. For example, x4 dilute inoculum combined with low light supported granulation under the different shear conditions utilized. However, x4 dilution inoculum with high light and high shear did not support granulation. This observed disparity in applied conditions suggests that OPG granulation ensues only with favorable interaction of variable induced energy pressures coupled with biological response selecting for spheroidal aggregates. Multi-regression analysis on temporal changes in the ratio of sludge volume index for 5 min to 30 min settling, a metric for granulation, confirmed the intercorrelation of these energy inputs on OPG granulation. This granulation scheme, dependent on goldilocks interaction of selection pressures, can potentially be extended to other granules applied in wastewater treatment.

INTRODUCTION

Phototrophs harness solar energy to power synthesis of biomolecules constituting the basic production system for the biosphere.[1] Phototrophic microbes are often integrated into different architectural assemblages in their environmental niches.[2] While these assemblages can have deleterious environmental impacts[3] and cause infrastructure damage,[4] they can also be beneficially utilized for anthropogenic applications, such as photogranular wastewater treatment.[5–7]

Granular sludge consists of self-immobilized microbial consortia with high density and spheroidal profiles. Each granule is effectively a 'micro-reactor' in which biochemical transformations occur. The granules' compact structure can also withstand high-strength wastewater and shock loadings.[8,9] These characteristics facilitate higher retention of biomass, giving cost and space savings compared to conventional wastewater treatment operations.[10,11] Anaerobic granules consist of co-operative methanogenic, acetogenic, and hydrolytic fermentative trophic groups.[10] Aerobic granules, on the other hand, have a microbial consortium comprising aerobic heterotrophic bacteria and nitrifying bacteria on their outer layers with facultative, anaerobic bacteria in their cores.[12] While the apparent disparity in microbial dominance between the above granules is dependent on environmental niche occupied, microbial colonialization evolves along a spatial gradient, resulting in generic layered granular structures. These self-immobilized granular bioaggregates can thus be considered homologs, similar in structure but differing in microbial species dominance.

Oxygenic photogranules (OPG) bear resemblance to this ubiquitous granular morphology.[13–18] The microbial community in OPGs consists of filamentous cyanobacteria and algae species dominating the phototrophic outer layer with light exposure while non-phototrophic bacteria dominate the inner core.[16–18] Unlike other granules reported,[19–23] OPGs have been cultivated and applied in illuminated reactors without supplemental aeration.[8,16–20] Presently the protocol for the generation of OPGs involves inoculating activated sludge in glass vials with light under hydrostatic conditions.[13–18] The setup usually results in the generation of a single OPG aggregate in each vial that can subsequently be introduced into a reactor for wastewater treatment.[13]

Selection pressures reported to enhance the formation of other granules[19,20,23–25] can also be inferred for OPGs. Sequencing batch reactor (SBR) operation of OPGs, with a 10 min settling period,[13] effectively retains rapidly-settling biomass. This settling-time based selection together with SBR cycle lengths (4 h)[13] induced hydraulic selection pressure (HSP).[25,26] It has been reported that long settling and cycle periods induced minimal HSP and hence did not promote the propagation of aerobic or nitrifying granules, while too short settling times resulted in washout of microbes and small granules hence no granulation.[23,24] Therefore, for successful granulation, the rate of removal of unsettled granules via HSP control should consider their growth rate ($\mu_{granules}$) to ensure retention of juvenile granules and sufficient biomass for functionality.

Feast and famine selection pressure inherent in SBR operations has also been reported as necessary to granulation.[26] Granular systems, including OPG reactors,[13] are predominantly operated in this scheme.[11,20] SBR cycling operation fosters substrate diffusion gradients into the granular matrix[27] with convective mass transport also distributing substrates in bulk fluid and into the granules through their porous structure.[28,29] Furthermore, OPG reactors were configured with operational cycling of dark and light periods creating feast and famine conditions for ‘light-substrate’.[13] For OPGs developed under hydrostatic conditions, famine conditions persisting initially in activated-sludge inoculum are followed by a feast state due to biomass decay.[14,15] In these conditions, compaction of activated-sludge inoculum was promoted and light-induced phototrophic enrichment resulted in OPG development.[14–16]

The presence of shear pressure in granular systems serves to suspend the biomass and distribute bulk substrate flux. Shear is also essential for sizing and 'shaping' granules, with higher shear resulting in smaller and more spherical aggregates.[30,31] Shear force increases hydrophobicity and particle density while also aiding in initiating and enhancing collision of particles in the fluid media.[31] Agitation in OPG reactors, provided by mechanical mixing, not only has similar influences but also critically facilitates the interaction of the granules with the light substrate. Light supplied at the surface of reactors penetrates the fluid media and decays per Beer-Lamberts law.[32] The turbidity[33] in the reactor bulk matrix limits light penetration necessitating the suspension of OPGs to 'see' light substrate.[34] For cyanobacteria which form the structural backbone of OPGs,[14] growth is strongly correlated to light intensity and weakly to carbon assimilation in a growth optimization strategy.[35] Mixing is therefore essential to ensure optimal interaction of OPGs with light to sustain granular functional and structural integrity.

The ubiquity of granulation and selection pressures promoting granule formation and function led to a hypothesis that the formation of seed OPGs from activated sludge should also occur under hydrodynamic conditions. We likewise hypothesized that granulation of OPGs occurs within a 'goldilocks zone' due to the interaction of chemical energies, shear pressure, and light energy in varying magnitudes. This study aims to examine these two hypotheses by conducting matrices of batch experiments with varying energy flows. If successful, the formation of OPGs under hydrodynamic conditions would be a preferred seeding protocol to hydrostatic cultivation. Nevertheless, the work associated with the second hypothesis may explain why OPGs, and potentially other granules, would still occur under limited sets of environmental conditions.

MATERIALS AND METHODS

Experimental set-up

A jar-test rig mixer was used to induce mixing in batch reactors. The mixer's variable speed drives were calibrated to run at speeds of 20 rpm, 50 rpm, and 80 rpm. The paddle-blade impellers had diameter of 5 cm, width 2.9 cm and were set at a clearance of 5 cm from the vessel bottom. Clear cylindrical-glass jars (1 L) were used for the experiment with an operating volume of 800 mL. The 20 rpm, 50 rpm, and 80 rpm mixing speeds induced theoretical shear stresses[36] of 0.01 N m^{-2} (11 s^{-1}), 0.04 N m^{-2} (39 s^{-1}), and 0.07 N m^{-2} (73 s^{-1}), respectively–see supporting information for more hydrodynamic property information. Batches were operated under three light intensities of 6.4±1 KLux, 12.7±1 KLux, and 25±1 KLux, using 9 W LEDs (EcoSmart, daylight 5000 K) with a luminosity of 840 Lumens. These light conditions are equivalent to photosynthetic flux densities of 117, 216, and 450 μmol m^{-2} s^{-1}, respectively, and were provided continuously for a duration of 8 days. There was no supplemental aeration in all batch systems.

Reactor seeding

We collected activated-sludge inocula from a local wastewater treatment plant on three different days for the current study. The collected activated sludge had mixed-liquor suspended solids (MLSS) of 5300 mg/L, 3900 mg/L, and 4400 mg/L for 20 rpm, 50 rpm, and 80 rpm sets, respectively. The biomass had an average ratio of 85% between volatile suspended solids (VSS) and MLSS. This inoculum was diluted with deionized water giving x4, x2 and x1 dilution inocula. The batch reactors were then seeded and capped to minimize evaporation. Each batch ensemble was set up with a constant mixing speed with different light intensities and dilution (e.g., 9 batches for 80 rpm ensemble combined with three light conditions and three dilutions). Total 27 batches, each in duplicate, were operated (Table 1).

Analytical methods

Sludge volume index (SVI) after 5 min and 30 min settling of biomass, SVI_5 and SVI_{30}, was determined based on Standard Methods (2710D).[37] Total and volatile suspended solids (TSS and VSS), chlorophyll pigments, and dissolved oxygen (DO) were either measured or determined following a designated method in Standard Methods.[37]

Imaging analysis and microscopy

We periodically collected samples (5 mL) of mixed biomass in Petri dishes and obtained high-resolution images. Image pro®v10 software (MEDIA CYBERNETICS) was utilized to characterize for particle sizes and number. A Weibull distribution was used to describe the particle size distribution (PSD).[38] Additionally, we conducted light microscopy (EVOS FL Color AMEFC-4300) using bright field and epifluorescence (RFP light cube-532 excitation/590 Emission) to characterize changing morphology and microbial composition.[17] Enrichment of cyanobacteria expected with OPG granulation results in golden-orange fluorescence due to the cyanobacteria's phycobiliproteins, specifically phycoerythrin.[39]

Statistical analysis

Minitab (Minitab v.17) and Excel (2010) were applied for all statistical analysis. The significance of the results was determined at the 0.05 probability level. A metric SVI_5/SVI_{30} ratio was used to describe temporal settleability[40] of samples. Multiple regression models (least squares) were fit to the change in SVI_5/SVI_{30} ratio data for day 6 and day 8 using the experimental parameters (light, mixing, and dilution) as predictor variables. Models were developed without (M) and with (M^i) parameter interactions. More details on the model setup are presented in supporting information. Pearson correlation was used to evaluate the correlation between variables.

RESULTS

Generation of OPGs by hydrodynamic batches using activated-sludge inoculum

Granular aggregates appeared in several batches operated with different magnitudes of mixing, light, and inoculum concentration (Figure 1). The images of 5 mL grab-sample biomass on day 8 showed that batches with lower mixing speeds (20 rpm and 50 rpm) and higher biomass dilutions (x4 and x2) across all three light conditions yielded granular aggregates. Granular aggregates were observed in these sets by day 5. Under 80 rpm mixing, mainly one set (x4, 6.4 KLux) was discernable for granule formation. Furthermore, all batches conducted with undiluted (x1) inoculum did not reveal identifiable granules, regardless of any mixing and light conditions provided.

Light microscopy confirmed that granules formed in these hydrodynamic batches were analogous to OPGs cultivated under hydrostatic conditions or those produced in reactor operation seeded with hydrostatically-formed OPGs (Figure 2; Figure S1). Like previously reported OPGs,[14,15,41] the granules' outer surface was dominated by filamentous cyanobacteria that formed an interwoven mat-like structure. Autofluorescence microscopy also led to clear visualization of these filamentous cyanobacteria due to their phycobilin pigment. The flexing and gliding motility of filamentous cyanobacteria was observed, indicating that they belong to the subsection III cyanobacteria, which are different from other filamentous cyanobacteria (i.e., the subsections IV-V) that are non-motile and also undergo cell differentiation.[42,43] The enrichment of the subsection III cyanobacteria, or "Oscillatoriales" in the traditional sense,[42] is well documented from OPGs cultivated under hydrostatic conditions and reactor operation.[14]

Evolution of particle sizes

We investigated the change in particle sizes that occurred in the hydrodynamic batches. An increase of the consortia particle concentration around the mean size was observed under all conditions with 20 rpm agitation (Figure 3a-c; Table S1). The mean particle sizes for x4 and x2 dilution ensembles, most of which showed the formation of OPGs (Figures 1, 2), changed from an average of 0.08 mm and 0.06 mm both to 0.15(±0.004) mm, while the mean size of undiluted ensemble increased from an average of 0.06 mm to 0.11(±0.004) mm. The increase in mean particle size was also accompanied by positively skewed distributions.

For 50 rpm sets (Figure 3d-f; Table S1), the mean particle size exhibited decreases for x4 and x1 dilutions and an increase for x2 dilutions. For the x4 dilution ensemble, the mean particle size decreased from 0.16 mm to 0.14(±0.019) mm. The mean particle size for x2 dilutions increased from 0.13 mm to 0.15(±0.008) mm, while those of undiluted ones decreased from 0.11 mm to 0.10(±0.01) mm. While PSD was observed to shift towards smaller sizes for the entire 50 rpm batches, the sets with x4 and x2 dilutions in which OPGs appeared exhibited more significant positive skews towards larger sizes. The overall decrease in both mean and median size for the 50 rpm ensemble can be attributed to particle breakage and detachment resulting from higher mixing-induced particle-particle collisions.[24,31] However, the positive skews observed in higher-dilution sets indicate an increase in the concentration of larger particle sizes, including granules (Figures 1, 2). This increase in sizes for 50 rpm suggests a microbially driven aggregation withstanding the shear limitations.[44]

The 80 rpm ensemble had an average initial mean particle size of 0.12(±0.002) mm. This mean was conserved at 0.12(±0.026) mm for x4 dilution while decreasing to 0.10(±0.008) mm and 0.08(±0.018) mm for x2 and x1 dilutions, respectively. Compared to day 0 samples, most 80 rpm sets experienced a shift towards smaller PSD. It is worth noting that PSD became significantly positively skewed in x4 dilutions with two lower light conditions, indicating increase in the concentration of larger particle sizes.

Assessment of settleability with SVI

The SVI is used to assess the ease of solids separation in wastewater treatment.[45] Activated sludge with effective settling typically shows SVI_{30} <150 mL/g.[46,47] OPGs from reactor operation have a reported average SVI_{30} of 53 mL/g.[13] Aerobic granules have a reported average SVI_5 of 88 mL/g[48,49] and algal-bacterial granules an average SVI_5 of 48 mL/g.[19]

The undiluted activated-sludge inoculum had an average SVI_5 of 221 mL/g (Figure 4) and SVI_{30} of 219 mL/g (Figure S2). Activated-sludge inocula with x4 and x2 dilutions showed average SVI_5 values of 798 mL/g and 432 mL/g and SVI_{30} of 235 mL/g and 246 mL/g, respectively. The significant increase of SVI_5 with dilution indicates poor settleability reflecting dilution-induced reduction of inter-particle interaction that diminishes flocculent (Type II) and hindered (Type III) settling effects in activated sludge.[28]

In 20 rpm and 50 rpm batches, all x4 dilution sets, all of which clearly showed the formation of OPGs (Figures 1, 2), exhibited clear decline in SVI_5 over the batch period. Except for one set, their terminal SVI_5, 65±5 mL/g, was comparable to that of aerobic granules and algal-bacterial granules. The incongruent 20 rpm-12.7 KLux-x4 batch, which clearly produced OPGs, had SVI_5 of 245 mL/g. The SVI result therefore indicates that the formation of granules in this set was not sufficient to lower SVI_5 for bulk biomass. This statement may also apply to the sets with 20 rpm, x2 dilutions under all light conditions, although granule formation was less conspicuous than the former batch. In contrast, batches with 50 rpm, x2 dilution showed SVI_5 proximate to or much less than 100 mL/g, indicating that these sets overall resulted in effectively settling biomass, including granules. The undiluted sets in 20 rpm and 50 rpm had little or marginal change in SVI_5 as well as high terminal SVI_5 values

(197±12 mL/g). The 80 rpm batch ensemble showed similar trend to the lower-mixing counterparts. However, only one set (80 rpm-6.4 KLux-x4), which showed the formation of OPGs, resulted in SVI_5 <100 mL/g. The settleability of this set was concordant with 6.4 KLux-x2 and 12.7 KLux-x2 batches with SVI_5 at 109 mL/g and 105 mL/g, respectively. As with 20 rpm and 50 rpm batches, there was little change in SVI_5 for undiluted sets at 80 rpm agitation.

Temporal change in SVI_5/SVI_{30} ratio

A temporal increase in settling velocities of biomass ensues with transition from floc to granular morphology, which translates to both decrease and convergence of the ratio of SVI_5/SVI_{30} over the batch period.[40] We hence examined this ratio as a characteristic metric for granulation (Figure 5).

Batches with x4 dilute inoculums in 20 rpm and 50 rpm mixing under all three light conditions, which produced easily observable OPGs, showed clear decreases in the SVI_5/SVI_{30} ratio over the 8-day experimental period. The decrease from the peak to the day 8 ratio in these six sets was by 60(±6)%. The counterparts in 80 rpm mixing showed an average decrease of 36(±8)%, while the set with 6.4 KLux, x4 dilution showed the highest difference at 50%.

The x2 dilutions in 20 rpm under all light conditions showed increases in SVI_5/SVI_{30} over the batch period. Hence, although OPGs were formed in these sets (Figure 1) and the settleability of biomass significantly improved, as seen with 66(±4)% decrease in SVI_{30} (Figure S2), both biomass morphology and SVI_5/SVI_{30} ratio data suggest that granulation in these sets was weaker than the x4 dilution sets. In 2x, 50 rpm sets where photogranules were formed under all light conditions, the SVI_5/SVI_{30} ratio decreased by day 8 after an initial increase. The average difference between the peak and the day 8 ratios was 48(±9)%. The 80 rpm, x2 dilution sets showed weaker convergence in the SVI_5/SVI_{30} ratio, compared to 50 rpm counterparts, or increased over the batch period.

Undiluted sets under all mixing and light conditions had increasing or unchanging SVI_5/SVI_{30}. These are the batches that also showed no or little change in SVI_5 during the experimental period (Figure 4). Furthermore, both macroscopic and microscopic examinations did not reveal observable granules. These results suggest that the undiluted batches were the least favourable for photogranulation to occur regardless of the conditions of mixing and light provided.

With the SVI_5/SVI_{30} ratio as a characteristic metric for granulation, multiple regression models[50] were fit to the change in SVI_5/SVI_{30} ratio data over the batch period to evaluate the significance and dependence on experimental parameters: light, mixing, and dilution (Table 2). Model fits without interactions (M) had R^2 of 49% on day 6 and 62% on day 8. On the other hand, the model results with parameter interactions (M^i) had R^2 of 56% and 70% for day 6 and day 8, respectively. Interaction of the predictors improved the model fit with lower deviation and better model fit for the data (R^2), suggesting significance of their interdependence on the SVI ratios. Moreover, improvements were also seen on the model fit adjusted for additional terms (R^2-adj) and in the model predictive capacity (R^2-pred). This improvement was, on average, 16% (std. dev 0.21) on day 6 and 11% (std. dev 0.01) on day 8 in the R^2 measures. On day 6 only mixing and dilution interactions showed significant impact on the SVI ratio changes and model-fit coefficients. However, day 8 showed significant interaction by all three parameters–model details are provided in supporting information. This can be attributed to continued illumination altering the phototrophic composition of biomass and impacting the settleability and granulation–the following section describes more about this.

Phototrophic enrichment

In 20 rpm sets, each batch was characterized by an initial decay phase with decreasing DO (Figure S3). This phase was followed by a phototrophic bloom seen with increasing chlorophyll pigments to day 4 (Figure 6a,b) and increase in DO indicating photosynthetic oxygenation. Between days 4 and 6, the three x4 dilution sets, which clearly supported granulation, showed a plateau phase for chlorophyll *a* but clear declining phase for chlorophyll *b*–chlorophyll *a* is the essential pigment for all phototrophs while chlorophyll *b* is accessory pigment associated with eukaryotic phototrophs.[51] This result, also with microscopic analysis (Figure 2; Figure S1), therefore suggests enrichment of cyanobacteria in these batches. Between days 6 and 8, an increase in both chlorophyll *a* and *b* was observed, inferring increased population of microalgae.[13,15,51] In the other 20 rpm sets, a consistent increase of chlorophyll *a* and *b* ensued between days 4 to 8, in the majority of sets, suggesting prevalence of microalgal enrichment.[13,15,51]

For sets under 50 rpm agitation, a general increase in chlorophyll *a* by day 4 was accompanied by minor changes in chlorophyll *b* (Figure 6c,d). These chlorophyll trends allude to cyanobacterial enrichment in the ensemble. The chlorophyll *a* increased beyond day 4 to the end of the experiment, generally increasing with dilution to day 6. Moreover, chlorophyll *a* in the x4 and x2 sets, those producing OPGs, were clustered higher than non-granulating undiluted sets by day 6–one exception was the 6.4 KLux-2x batch. Chlorophyll *b* concentrations increased with dilution and light intensity after day 4 in contrast to 20 rpm sets, which primarily increased after day 6. These faster increases, an indicative of faster microalgal growth, can be ascribed to elevated light energy interactions per particle concentration from higher agitation.

Under 80 rpm, both chlorophyll *a* and *b* concentrations in most sets had marginal increases up to day 4 and further increases up to day 8 (Figure 6e,f). Analogous to the 50 rpm ensemble, the increase was proportional to dilution alluding to light penetration expediency within the batch vessels. The pigment concentrations in x2 and x1 dilutions increased with light intensity but not in x4 dilution sets which had potentially higher variability in light interactions. In this 80 rpm set, the trends in chlorophyll *a* concentrations were strongly correlated to that of chlorophyll *b* with an average r=0.97, indicating that microalgal growth was dominant in these batches. Basically, only one set which had the lowest light, and the lowest amount of biomass rendered the formation of OPGs (Figure 1).

DISCUSSION

Current research on granule-based wastewater treatment focuses on understanding granules' operational and functional characteristics to improve their engineering application.[40,52–54] For photogranular biomass, photosynthesis presents additional functional complexity due to its interaction with light.[1,22,55] The phototrophic microbes are essential for either granular structure such as in algal-bacterial aggregation with aeration[19–21] or both the structure and function for OPGs with self-aeration.[13–15,18] In the latter, maintaining functional integrity involves balancing the photosynthetic rate generating oxygen and the microbial consortia respiration rates consuming oxygen for organic matter removal and nitrification.

This study examined the potential for hydrodynamic granulation of OPGs from activated-sludge inoculum, which was previously generated under hydrostatic conditions.[14–16] While different combinations of conditions were examined, the batch sets having 20 rpm and 50 rpm mixing, combined with x4 and x2 dilute activated-sludge inoculum and the three different light conditions tested were found to be amenable for formation of OPGs (Figures 1, 2). These results present not only an additional way to produce seed OPGs but also opportunities for rapid (5-8 days) and bulk development of OPGs compared to the previous singular generation using hydrostatic cultivation (21 days).[15]

We showed that high agitation rates with 80 rpm mixing (0.07 N m^{-2}; 73 s^{-1}) resulted in a decline of particle sizes and curtailed aggregation in contrast to the lower agitation rates (Figure 3; Table S1). However, when combined with low-light intensity 6.4 KLux and x4 dilution, OPGs were formed even at this high shear. The batch sets with 20 rpm and 50 rpm mixing, on the other hand, resulted in granulation under a broader range of light intensities and dilution. While no OPGs were observed in hydrodynamic batches with undiluted inoculum regardless of any combination with mixing and light conditions provided, OPG granulation has occurred with undiluted activated-sludge inoculum under negligible kinetic energy (i.e., hydrostatic photogranulation).[14–16] These variable experimental outputs, therefore, indicate a granulation promoting confluence of diverse magnitudes of applied variables (i.e., kinetic, biochemical, and light energies).

Various investigators have reported on the importance of shear as a core selection pressure for granulation.[26,30,31] Hydrodynamic forces distribute the mass flux within the reactor and initiate particle-particle interaction with induced shear sculpting the resultant three-dimensional structure.[31] Moreover, the increase in hydrophobicity induced by strong shear is essential for the initial cell-to-cell contact as it reduces the surface free Gibbs energy of the cells, resulting in their separation from the liquid phase.[26,31,49] The changes in biomass morphology and the decrease and convergence of SVI_5/SVI_{30} ratio indicate sustained aggregation of biomass in the lower shear environment compared to the high shear rate 80 rpm sets. Propagation of OPGs has been reported in reactor operations with a calculated shear rate of 38 s^{-1},[13] comparable to 50 rpm conditions employed in this study. This similarity suggests an ideal shear range for granulation in a hydrodynamic environment.

We also examined the effect of shear on photogranulation from the perspective of particle size distribution. The 80 rpm mixing in this study resulted in a calculated Eddy length scale[56] of 119 μm, comparable to or smaller than the inoculum's mean and median particle size of 118 μm and 220 μm, respectively (Table S1). Enhanced particle collisions and dissipation of kinetic energy,[57] therefore, most likely limited aggregation in the 80 rpm ensemble and decreased the bulk consortia size. This shear effect will be particularly enhanced in undiluted sets because increasing solids concentration (mean MLSS 1061 mg/L and 4523 mg/L in x4 and x1 dilutions, respectively) distorts the viscosity of the bulk fluid transforming its rheology from a Newtonian dominated flow into a particle-particle interaction flow suspension.[58,59] A higher viscosity in undiluted sets would therefore result in higher shear stress on particles compared to diluted sets, which is supported by PSD trends (Figure 3) and average mean and median particle sizes among the 80 rpm ensemble (Table S1)–this trend also holds true for the lower mixing sets. Nevertheless, some granulation observed under 80 rpm mixing can be attributed to the microbial resistance to particle interactions and shear stress,[44] especially with dilution. For 50 rpm batches, an Eddy length of 164 μm was determined with a mean inoculum particle size of 132 μm and a median of 220 μm. On the other hand, the 20 rpm set had an Eddy scale of 301 μm compared to the inoculum mean size of 72 μm and median 153 μm. The higher length scales of shear energy dissipation compared to particle sizes and a reduced particle-particle collision could explain the enhanced granulation in the 20-50 rpm ensembles.

In OPGs, the light substrate is an essential source of energy for photosynthesis to occur. Among various phototrophs, enrichment of the subsection III filamentous cyanobacteria possessing motility[42,43] and their entanglement have been postulated to be responsible for OPG development.[16,17] In the batch operation adopted, the utility of light substrate is a function of light intensity provided as well as both dilution and agitation. Phototrophic enrichment showed a high sensitivity to increasing light intensity (Figure 6). Inoculum dilution likewise allows for penetration of light, increasing light-biomass interaction compared to undiluted sets at the same mixing speed. Supporting this, the change in mean particle sizes had a high positive correlations to the light intensity (r >0.85) and dilution (r >0.92) across all mixing speeds. In addition, a higher mixing speed increases the incidence of light exposure at the same light intensity. Consequently, the proportion of phototrophic enrichment generally increased with both the dilution and mixing speed under the same intensity of light.

However, no OPGs were formed in high-shear and high-light substrate conditions (80 rpm-25 KLux) (Figure 1). The high-energy inflow from high agitation and light intensity were found to favor microalgae growth rather than filamentous cyanobacteria, seen with both microscopy (Figure 2) and the trend of chlorophyll *a* and *b* concentrations (Figure 6). Algae are known for higher shear tolerance compared to both cyanobacteria and dinoflagellates,[44] which may explain the persistence of algae under the 80 rpm agitation. Moreover, microalgae are tolerant and can adapt to high-intensity light,[60] whereas filamentous cyanobacteria are well known for their photophobic characteristic.[61] Hence, the lack of granulation of OPGs in these 'high-energy' sets could be due to repressed growth of cyanobacteria, which may arise from light induced photoinhibition and shear-induced limitation.

Despite the different morphologies of biomass, both activated sludge and granular biomass systems employ similar inputs, namely, agitation, a wastewater stream, and a microbial consortium. In conventional activated sludge operations for wastewater treatment, no spontaneous granule formation has been reported to date. However, altered operational conditions have resulted in the formation of granular biomass using activated-sludge inoculum. [14,15,48,52] Moreover, similar inputs exist in other environments, such as in waterways, where niche colonization takes the morphology of mats and biofilms.[2] Thus, despite the prevalence of analogous conditions, the form and interactions of those conditions likely select for enhancement of different phenotypes.[54,62] It thus seems evident that operational or ecological conditions inducing specific bio-physiological response are responsible for granulation.

It can be surmised that granulation of OPGs, or any granulation, occurs under the influence of macro inputs coupled with biological responses. Results presented with OPG granulation in this study indicate the existence of multiple granulation frontiers with different combinations of energy inputs: light, shear, and biochemical energies. This statement also applies to a previous discovery that granulation of OPGs occurs even in a hydrostatic environment, which is considered a rare phenomenon.[16–20] The various ensembles of energy can be presented as a 'zone of granulation interactions' (Figure 7). When these 'goldilocks conditions' are achieved, a bio-structural response is expected to ensue favouring spheroidal structures and enhancing selection of aggregating characteristics of filamentous cyanobacteria for OPGs. Similar optimal interaction of shear and substrate energies has recently been reported from 2-D modelling for aerobic granules. The selection pressure strategies applied influenced substrate availability which was shown to promote granulation.[54]

We propose that particle-particle attachment coupled with ecological associations as microbes seek a survival niche[63] occurs at the onset of granulation. This initial aggregation is compounded by increasing sizes of the micro flocs due to microbial growth, particle adherence, and filamentous entanglement.[15,31] Thereafter, microbial translocation aided by cell motility and dominance in response to persisting environmental conditions,[16] seem to occur in tandem with granular growth. Current approaches seek to identify discrete environmental selection conditions within this granulation enabling zone.[9] The outcome of this study indicates the existence of a wide array of 'granulating' conditions. A systems-based broad perspective, such as conditional flux-based analysis,[62] can be used to identify the tradeoffs for operational conditions selecting for granulation. Further research is necessary to develop appropriate formalism and to identify similarities in the biological response of different granules morphologies.

CONCLUSION

Different morphologies have been observed between similar microbial populations and comparable environmental stresses of varying magnitudes. These suggest potential links between the magnitudes and interactions and resulting bio-physiological structures. This study shows activated sludge which experienced shear, light and nutrient (substrate) pressure from dilution was transformed into OPGs by varying the magnitudes of these stresses. This presents potential opportunities for in-basin transformation of conventional activated sludge floccular biomes into granular form by varying operational conditions. Further investigations and optimization are needed to translate the various process benefits enumerated for granular biomass in wastewater treatment.

ACKNOWLEDGEMENTS

We thank and acknowledge the contributions of Dr. Mike Dolan in refining microscopic imaging and the UMass-Amherst Statistical Consultation and Collaboration Services for guidance in statistical evaluation. This work was supported by the National Science Foundation [CBET1605424; IIP1919091]. We thank *Tomorrow Water* for generous gift donations on OPG research.

REFERENCES

1 J. Barber and B. Andersson, Too much of a good thing: Light can be bad for photosynthesis, *Trends Biochem. Sci.*, 1992, **17**, 61–66.

2 R. M. Donlan, Biofilms: Microbial life on surfaces, *Emerg. Infect. Dis.*, 2002, **8**, 881–890.

3 D. M. Anderson, P. M. Glibert and J. M. Burkholder, Harmful algal blooms and eutrophication: Nutrient sources, composition, and consequences, *Estuaries*, 2002, **25**, 704–726.

4 H. Jensen, C. A. Biggs and E. Karunakaran, The importance of sewer biofilms, *Wiley Interdiscip. Rev. Water*, 2016, **3**, 487–494.

5 X.-W. Liu, H.-Q. Yu, B.-J. Ni and G.-P. Sheng, in *Biotechnology in China I*, Springer, Berlin, Heidelberg, 2009, pp. 275–303.

6 D. A. Jasmine, K. B. Malarmathi, S. K. Daniel and S. Malathi, in *Smart Materials for Waste Water Applications*, 2016, pp. 379–398.

7 K. Milferstedt, J. Hamelin, C. Park, J. Jung, Y. Hwang, S.-K. Cho, K.-W. Jung and D.-H. Kim, Biogranules applied in environmental engineering, *Int. J. Hydrog. Energy*, 2017, **42**, 27801–27811.

8 S. S. Adav, D.-J. Lee, K.-Y. Show and J.-H. Tay, Aerobic granular sludge: Recent advances, *Biotechnol. Adv.*, 2008, **26**, 411–423.

9 Q. Zhang, J. Hu and D.-J. Lee, Aerobic granular processes: Current research trends, *Bioresour. Technol.*, 2016, **210**, 74–80.

10 S. McHugh, C. O'Reilly, T. Mahony, E. Colleran and V. O'Flaherty, Anaerobic Granular Sludge Bioreactor Technology, *Rev. Environ. Sci. Biotechnol.*, 2003, **2**, 225–245.

11 R. Noppeney, About the Nereda Wastewater Treatment Process, https://www.royalhaskoningdhv.com/en-gb/nereda/nereda-wastewater-treatment%20technology, (accessed 19 September 2018).

12 D. Gao, L. Liu, H. Liang and W.-M. Wu, Aerobic granular sludge: characterization, mechanism of granulation and application to wastewater treatment, *Crit. Rev. Biotechnol.*, 2011, **31**, 137–152.

13 A. S. Abouhend, A. McNair, W. C. Kuo-Dahab, C. Watt, C. S. Butler, K. Milferstedt, J. Hamelin, J. Seo, G. J. Gikonyo, K. M. El-Moselhy and C. Park, The Oxygenic Photogranule Process for Aeration-Free Wastewater Treatment, *Environ. Sci. Technol.*, 2018, **52**, 3503–3511.

14 K. Milferstedt, W. C. Kuo-Dahab, C. S. Butler, J. Hamelin, A. S. Abouhend, K. Stauch-White, A. McNair, C. Watt, B. I. Carbajal-González, S. Dolan and C. Park, The importance of filamentous cyanobacteria in the development of oxygenic photogranules, *Sci. Rep.*, 2017, **7**, 17944.

15 W. C. Kuo-Dahab, K. Stauch-White, C. S. Butler, G. J. Gikonyo, B. Carbajal-González, A. Ivanova, S. Dolan and C. Park, Investigation of the Fate and Dynamics of Extracellular Polymeric Substances (EPS) during Sludge-Based Photogranulation under Hydrostatic Conditions, *Environ. Sci. Technol.*, 2018, **52**, 10462–10471.

16 K. Stauch-White, V. N. Srinivasan, W. Camilla Kuo-Dahab, C. Park and C. S. Butler, The role of inorganic nitrogen in successful formation of granular biofilms for wastewater treatment that support cyanobacteria and bacteria, *AMB Express*, , DOI:10.1186/s13568-017-0444-8.

17 A. A. Ansari, A. S. Abouhend and C. Park, Effects of seeding density on photogranulation and the start-up of the oxygenic photogranule process for aeration-free wastewater treatment, *Algal Res.*, 2019, **40**, 101495.

18 C. Park and S. Dolan. Algal-sludge granule for wastewater treatment and bioenergy feedstock generation, US PATENT, US 10,189,732 B2, 2019, 11.

19 J. S. M. Ahmad, W. Cai, Z. Zhao, Z. Zhang, K. Shimizu, Z. Lei and D.-J. Lee, Stability of algal-bacterial granules in continuous-flow reactors to treat varying strength domestic wastewater, *Bioresour. Technol.*, 2017, **244**, 225–233.

20 Q. He, L. Chen, S. Zhang, R. Chen, H. Wang, W. Zhang and J. Song, Natural sunlight induced rapid formation of water-born algal-bacterial granules in an aerobic bacterial granular photo-sequencing batch reactor, *J. Hazard. Mater.*, 2018, **359**, 222–230.

21 B. Zhang, P. N. L. Lens, W. Shi, R. Zhang, Z. Zhang, Y. Guo, X. Bao and F. Cui, Enhancement of aerobic granulation and nutrient removal by an algal–bacterial consortium in a lab-scale photobioreactor, *Chem. Eng. J.*, 2018, **334**, 2373–2382.

22 J. S. Arcila and G. Buitrón, Influence of solar irradiance levels on the formation of microalgae-bacteria aggregates for municipal wastewater treatment, *Algal Res.*, 2017, **27**, 190–197.

23 B. B K and M. G, Influence of three selection pressures on aerobic granulation in sequencing batch reactor, *Indian J. Chem. Technol. IJCT*, 2016, **22**, 241–247.

24 Y.-Q. Liu and J.-H. Tay, Fast formation of aerobic granules by combining strong hydraulic selection pressure with overstressed organic loading rate, *Water Res.*, 2015, **80**, 256–266.

25 L. Qin, J.-H. Tay and Y. Liu, Selection pressure is a driving force of aerobic granulation in sequencing batch reactors, *Process Biochem.*, 2004, **39**, 579–584.

26 B. k. Bindhu and G. Madhu, Selection pressure theory for aerobic granulation – an overview, *Int. J. Environ. Waste Manag.*, 2014, **13**, 317–329.

27 Y. Li and Y. Liu, Diffusion of substrate and oxygen in aerobic granule, *Biochem. Eng. J.*, 2005, **27**, 45–52.

28 B.-M. Wilén, R. Liébana, F. Persson, O. Modin and M. Hermansson, The mechanisms of granulation of activated sludge in wastewater treatment, its optimization, and impact on effluent quality, *Appl. Microbiol. Biotechnol.*, 2018, **102**, 5005–5020.

29 T. Etterer and P. A. Wilderer, Generation and properties of aerobic granular sludge, *Water Sci. Technol.*, 2001, **43**, 19–26.

30 Y. Chen, W. Jiang, D. T. Liang and J. H. Tay, Structure and stability of aerobic granules cultivated under different shear force in sequencing batch reactors, *Appl. Microbiol. Biotechnol.*, 2007, **76**, 1199–1208.

31 Y. Liu and J.-H. Tay, The essential role of hydrodynamic shear force in the formation of biofilm and granular sludge, *Water Res.*, 2002, **36**, 1653–1665.

32 A. C. Brito and A. Newton, Measuring Light Attenuation in Shallow Coastal Systems, *J. Ecosyst. Ecography*, , DOI:10.4172/2157-7625.1000122.

33 C. L. Gallegos and K. A. Moore, in *Chesapeake Bay submerged aquatic vegetation water quality and habitat-based requirements and restoration targets: a second technical synthesis, edited by Batiuk, R.A*, EPA Chesapeake Bay Program, Annapolis, MD, 2000, pp. 35–54.

34 D. Krause-Jensen and K. Sand-Jensen, Light attenuation and photosynthesis of aquatic plant communities, *Limnol. Oceanogr.*, 1998, **43**, 396–407.

35 M. Jahn, V. Vialas, J. Karlsen, G. Maddalo, F. Edfors, B. Forsström, M. Uhlén, L. Käll and E. P. Hudson, Growth of Cyanobacteria Is Constrained by the Abundance of Light and Carbon Assimilation Proteins, *Cell Rep.*, 2018, **25**, 478-486.e8.

36 H. Furukawa, Y. Kato, Y. Inoue, T. Kato, Y. Tada and S. Hashimoto, Correlation of Power Consumption for Several Kinds of Mixing Impellers, *Int. J. Chem. Eng.*, 2012, **2012**, 1–6.

37 APHA, *Standard Methods for the Examination of Water and Wastewater*, APHA,AWWA,WEF, Washington: American Public Health Association, 2012.

38 L. Esmaeelnejad, F. Siavashi, J. Seyedmohammadi and M. Shabanpour, The best mathematical models describing particle size distribution of soils, *Model. Earth Syst. Environ.*, 2016, **2**, 1–11.

39 C. Carreira, M. Staal, M. Middelboe and C. P. D. Brussaard, Autofluorescence imaging system to discriminate and quantify the distribution of benthic cyanobacteria and diatoms: Imaging benthic photoautotrophs, *Limnol. Oceanogr. Methods*, 2015, **13**, e10016.

40 S. J. Sarma and J. H. Tay, Aerobic granulation for future wastewater treatment technology: challenges ahead, *Environ. Sci. Water Res. Technol.*, 2017, **4**, 9–15.

41 A. S. Abouhend, K. Milferstedt, J. Hamelin, A. A. Ansari, C. Butler, B. I. Carbajal-González and C. Park, Growth Progression of Oxygenic Photogranules and Its Impact on Bioactivity for Aeration-Free Wastewater Treatment, *Environ. Sci. Technol.*, 2020, **54**, 486–496.

42 W. B. Whitman, F. Rainey, P. Kämpfer, M. Trujillo, J. Chun, P. DeVos, B. Hedlund and S. Dedysh, Eds., *Bergey's Manual of Systematics of Archaea and Bacteria*, Wiley, 1st edn., 2015.

43 L. J. Stal, in *Algae and Cyanobacteria in Extreme Environments*, ed. J. Seckbach, Springer Netherlands, Dordrecht, 2007, vol. 11, pp. 659–680.
44 C. Wang and C. Q. Lan, Effects of shear stress on microalgae - A review, *Biotechnol. Adv.*, 2018, **36**, 986–1002.
45 C. M. Bye and P. L. Dold, Sludge volume index settleability measures: effect of solids characteristics and test parameters, *Water Environ. Res.*, 1998, **70**, 87–93.
46 E. Amanatidou, G. Samiotis, E. Trikoilidou, G. Pekridis and N. Taousanidis, Evaluating sedimentation problems in activated sludge treatment plants operating at complete sludge retention time, *Water Res.*, 2015, **69**, 20–29.
47 Z. Li, P. Lu, D. Zhang, G. Chen, S. Zeng and Q. He, Population balance modeling of activated sludge flocculation: Investigating the influence of Extracellular Polymeric Substances (EPS) content and zeta potential on flocculation dynamics, *Sep. Purif. Technol.*, 2016, **162**, 91–100.
48 N. Derlon, J. Wagner, R. H. R. da Costa and E. Morgenroth, Formation of aerobic granules for the treatment of real and low-strength municipal wastewater using a sequencing batch reactor operated at constant volume, *Water Res.*, 2016, **105**, 341–350.
49 L. Zhu, J. Zhou, H. Yu and X. Xu, Optimization of hydraulic shear parameters and reactor configuration in the aerobic granular sludge process, *Environ. Technol.*, 2015, **36**, 1605–1611.
50 Minitab, Methods and formulas for Multiple Regression, https://support.minitab.com/en-us/minitab-express/1/help-and-how-to/modeling-statistics/regression/how-to/multiple-regression/methods-and-formulas/methods-and-formulas/, (accessed 20 June 2020).
51 H. L. Golterman, in *Physiological Limnology: An Approach to the Physiology of Lake Ecosystems*, Elsevier, 1975, vol. 2, pp. 233–247.
52 A. Sengar, F. Basheer, A. Aziz and I. H. Farooqi, Aerobic granulation technology: Laboratory studies to full scale practices, *J. Clean. Prod.*, 2018, **197**, 616–632.
53 Z. Yuanyuan, Z. Xuehong and Z. Wenjie, in *Proceedings of the AASRI International Conference on Industrial Electronics and Applications (2015)*, Atlantis Press, London, UK, 2015.
54 J. Wu, F. L. de los Reyes and J. J. Ducoste, Modeling cell aggregate morphology during aerobic granulation in activated sludge processes reveals the combined effect of substrate and shear, *Water Res.*, 2020, **170**, 115384.
55 R. M. Cory, C. P. Ward, B. C. Crump and G. W. Kling, Sunlight controls water column processing of carbon in arctic fresh waters, *Science*, 2014, **345**, 925–928.
56 P. M. Doran, in *Bioprocess Engineering Principles (Second Edition)*, ed. P. M. Doran, Academic Press, London, 2013, pp. 255–332.
57 J.-H. Tay, Q.-S. Liu and Y. Liu, The effects of shear force on the formation, structure and metabolism of aerobic granules, *Appl. Microbiol. Biotechnol.*, 2001, **57**, 227–233.
58 The influence of particles on suspension rheology, https://wiki.anton-paar.com/en/the-influence-of-particles-on-suspension-rheology/, (accessed 26 May 2019).
59 T. F. Ford, Viscosity-concentration, and fluidity-concentration relationships for suspensions of spherical particles in newtonian liquids, *J. Phys. Chem.*, 1960, **64**, 1168–1174.
60 G. M. Giacometti and T. Morosinotto, in *Encyclopedia of Biological Chemistry*, eds. W. J. Lennarz and M. D. Lane, Academic Press, Waltham, 2013, pp. 482–487.
61 R. W. Castenholz, Aggregation in a Thermophilic Oscillatoria, *Nature*, 1967, **215**, 1285–1286.
62 L. Guedes da Silva, S. Tomás-Martínez, A. Wahl and M. van Loosdrecht, *The environment selects: Modeling energy allocation in microbial communities under dynamic environments*, Preprint from bioRxiv, 2019.
63 A. M. Spormann, in *Bacterial Biofilms*, ed. T. Romeo, Springer Berlin Heidelberg, Berlin, Heidelberg, 2008, pp. 17–36.

Table 1. Experimental set-up with combinations of different conditions of light, mixing, and biomass dilution.

Light \ **Mixing**	20 rpm (0.01 N m^{-2})	50 rpm (0.04 N m^{-2})	80 rpm (0.07 N m^{-2})
6.4 KLux (117 µmol m^{-2} s^{-1})	x4, x2, and x1 dilution	x4, x2, and x1 dilution	x4, x2, and x1 dilution
12.7 KLux (216 µmol m^{-2} s^{-1})	x4, x2, and x1 dilution	x4, x2, and x1 dilution	x4, x2, and x1 dilution
25 KLux (450 µmol m^{-2} s^{-1})	x4, x2, and x1 dilution	x4, x2, and x1 dilution	x4, x2, and x1 dilution

Table 2. Multiple regression fit parameters for SVI_5/SVI_{30} ratio change.*

SVI day	Std. Dev (S)	R^2	R^2 (adj)	R^2 (pred)
Day 6 (M)	0.85	49.33%	46.35%	44.06%
Day 6 (M^i)	0.79	56.21%	53.63%	52.02%
Day 8 (M)	0.81	62.17%	59.94%	58.81%
Day 8 (M^i)	0.73	69.54%	67.11%	64.89%

*M: model results without interactions of experimental parameters (light, mixing, and dilution), M^i: results with experimental parameter interactions.

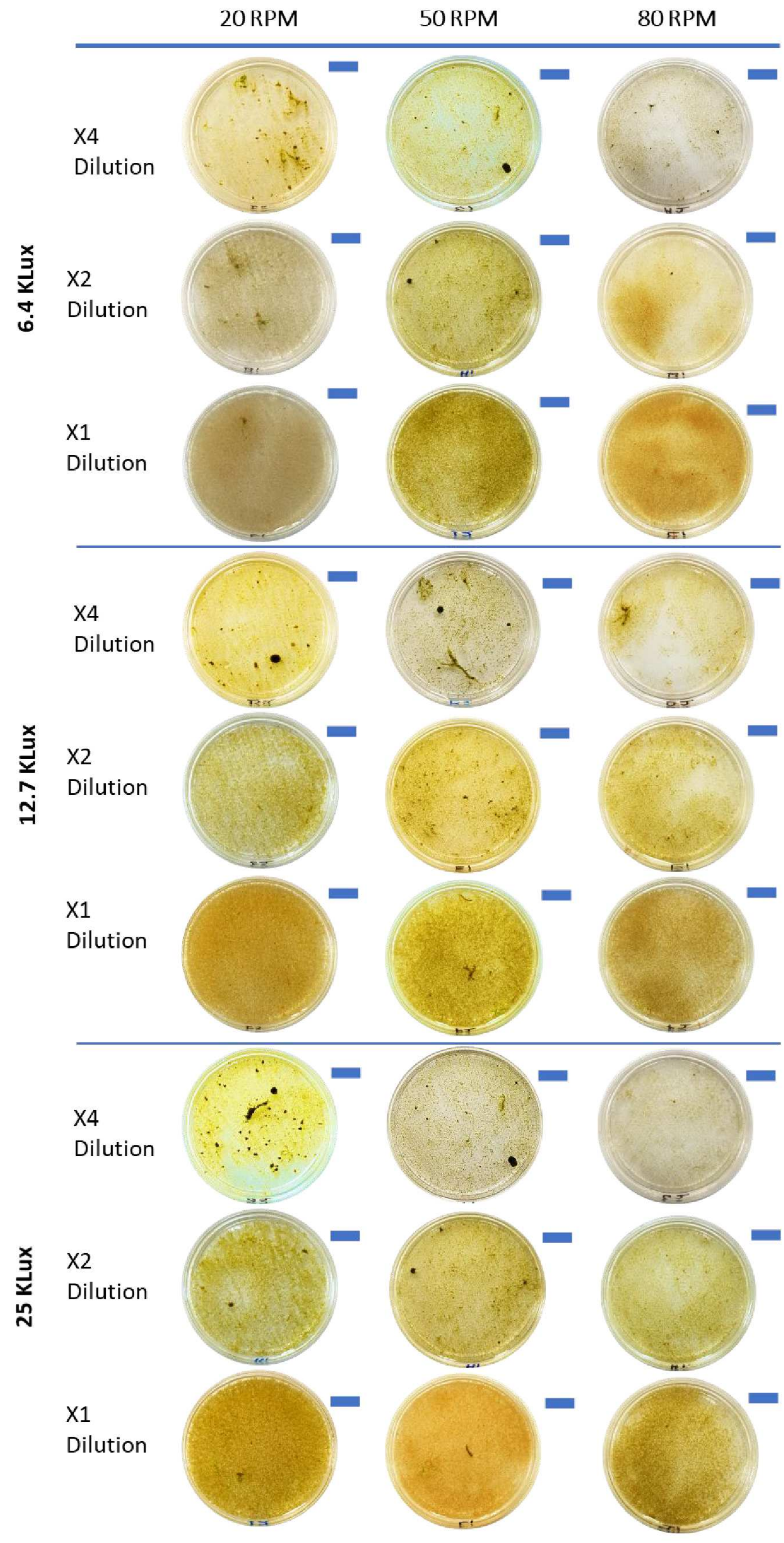
20 RPM
50 RPM
80 RPM
6.4 KLux
12.7 KLux
25 KLux
X4 Dilution
X2 Dilution
X1 Dilution

Figure 1. Petri dish images of 5 mL grab-sample mixed biomass from each batch reactor on day 8 run under different experimental conditions. Scale bars are 1cm.

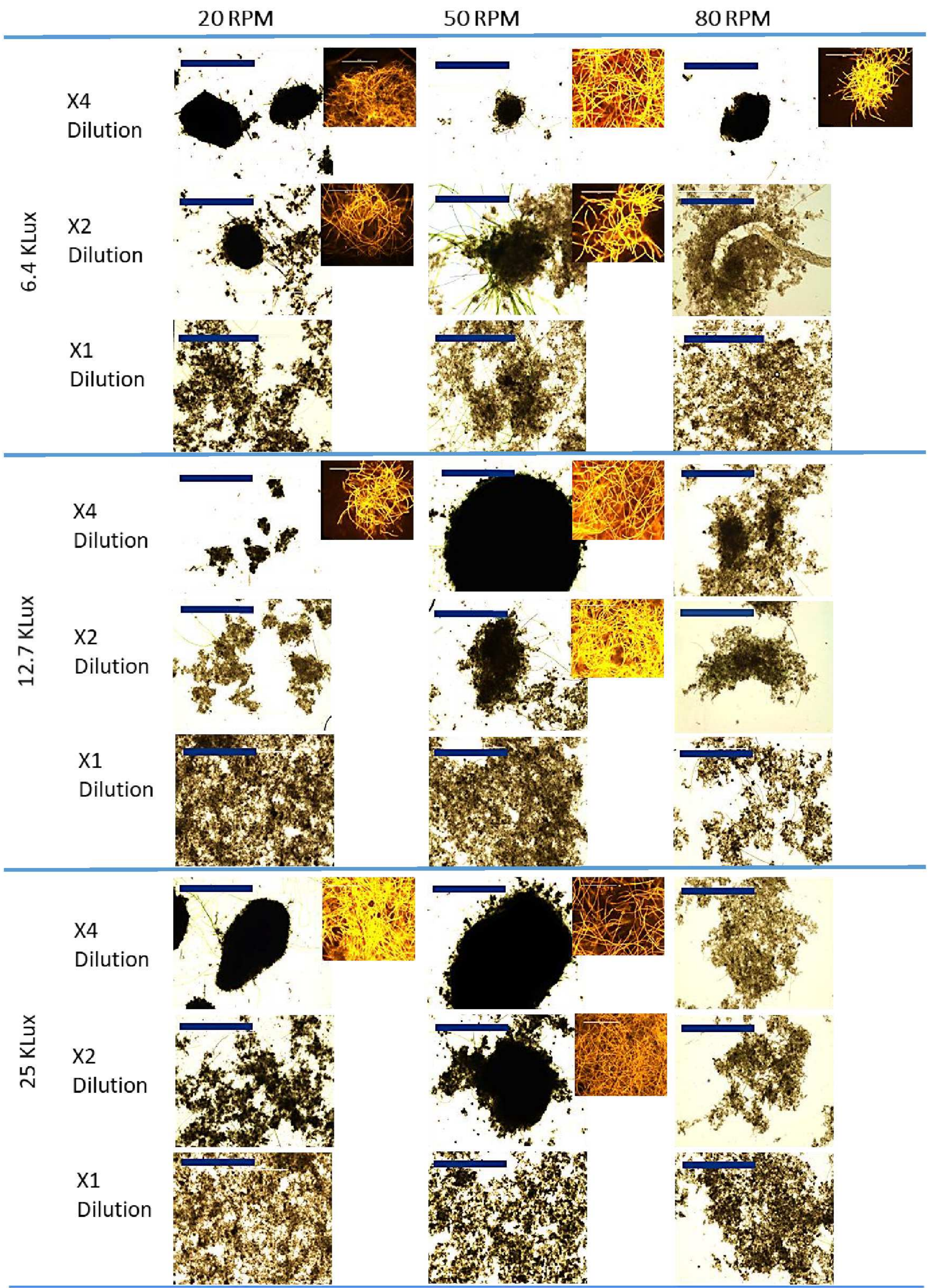

Figure 2. Day 8 light microscopic images of grab samples from 27 batches with different light, mixing, and dilution conditions. Scale bars are 2000 μm. Insets (not to scale) show phycobilin auto-fluorescence of filamentous cyanobacteria within photogranules.

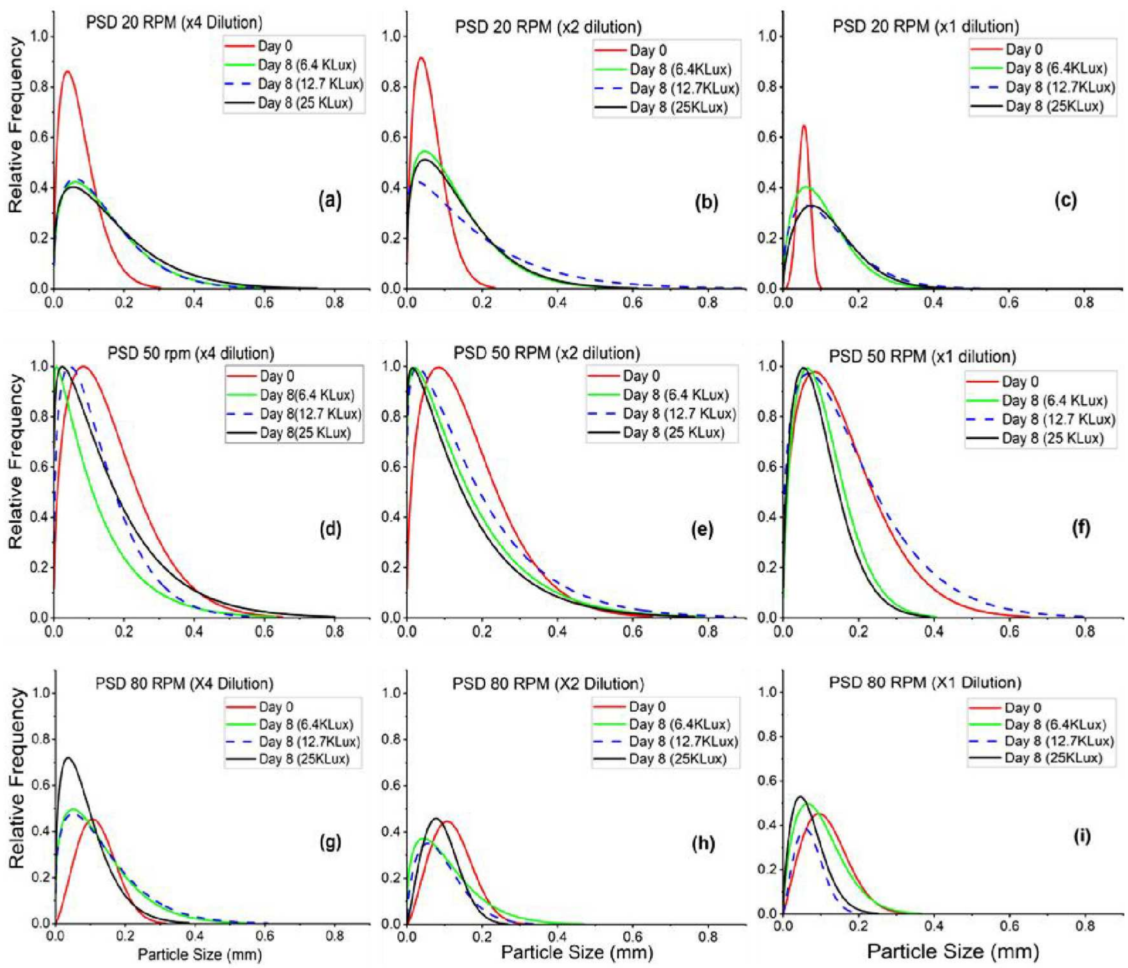

Figure 3. Particle size distribution (PSD) (Weibull distribution) showing the relative frequency of number of particles of each size to total number of particles within the sample (n >235). Top (a-c), middle (d-f), and bottom (g-i) panels are for batches mixed at 20 rpm, 50 rpm, and 80 rpm, respectively. Batches with each mixing speed had three dilutions of biomass inocula and three different light intensities.

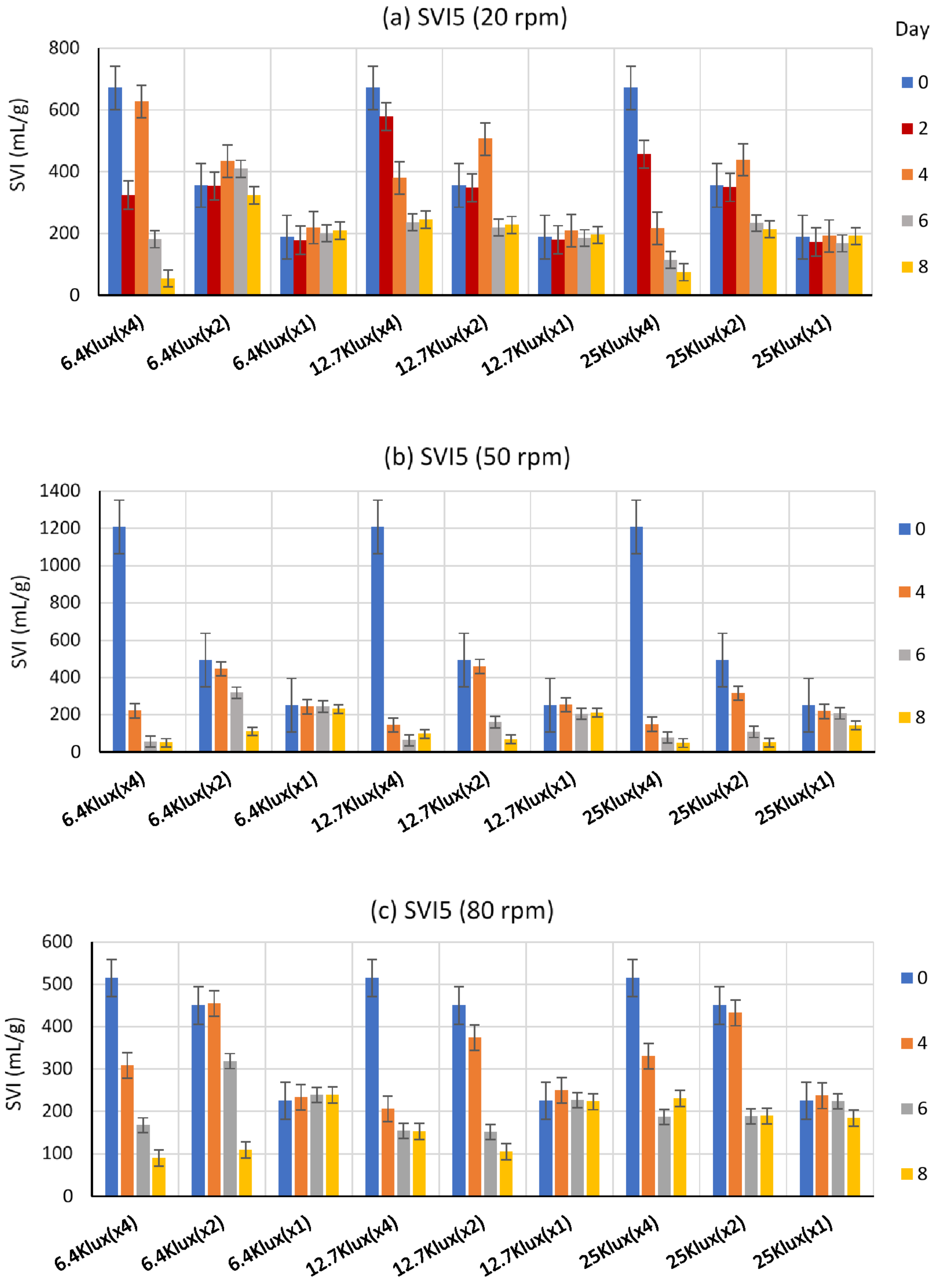

Figure 4. Five-min sludge volume index (SVI_5) of biomass in 27 batches over the experimental period from day 0 to day 8. Results are shown with different light intensities and biomass dilution under mixing conditions of a) 20 rpm, b) 50 rpm, and c) 80 rpm. Different vertical scales are used to reflect the disparity of initial SVI_5 magnitudes. Error bars represent the standard error of duplicate averages for each condition.

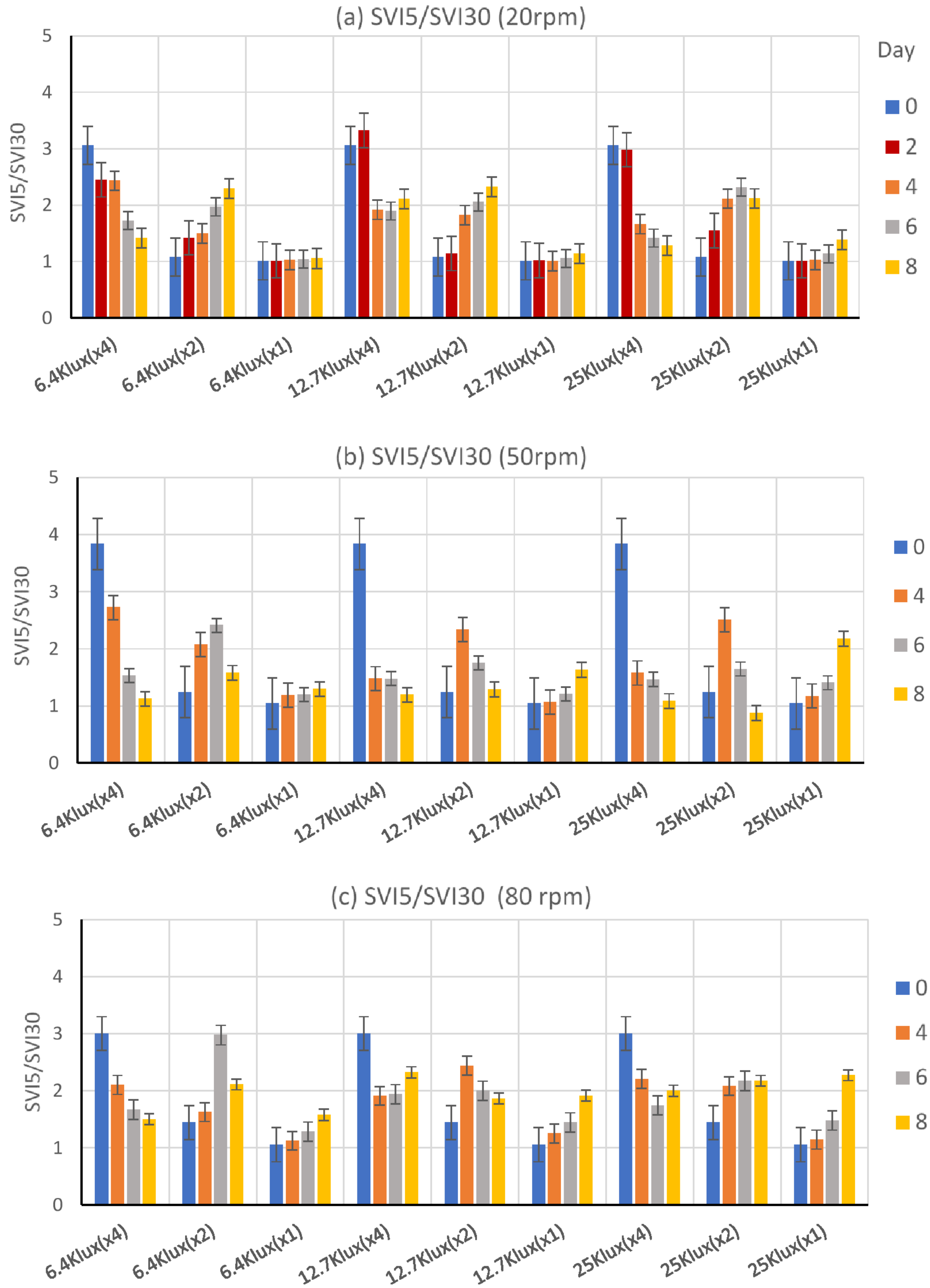

Figure 5. SVI_5/SVI_{30} ratio in 27 batches over the experimental period from day 0 to day 8. Results are shown with different light intensities and biomass dilution under mixing conditions of a) 20 rpm, b) 50 rpm, and c) 80 rpm. Error bars represent the standard error of each averaged ratio for each condition.

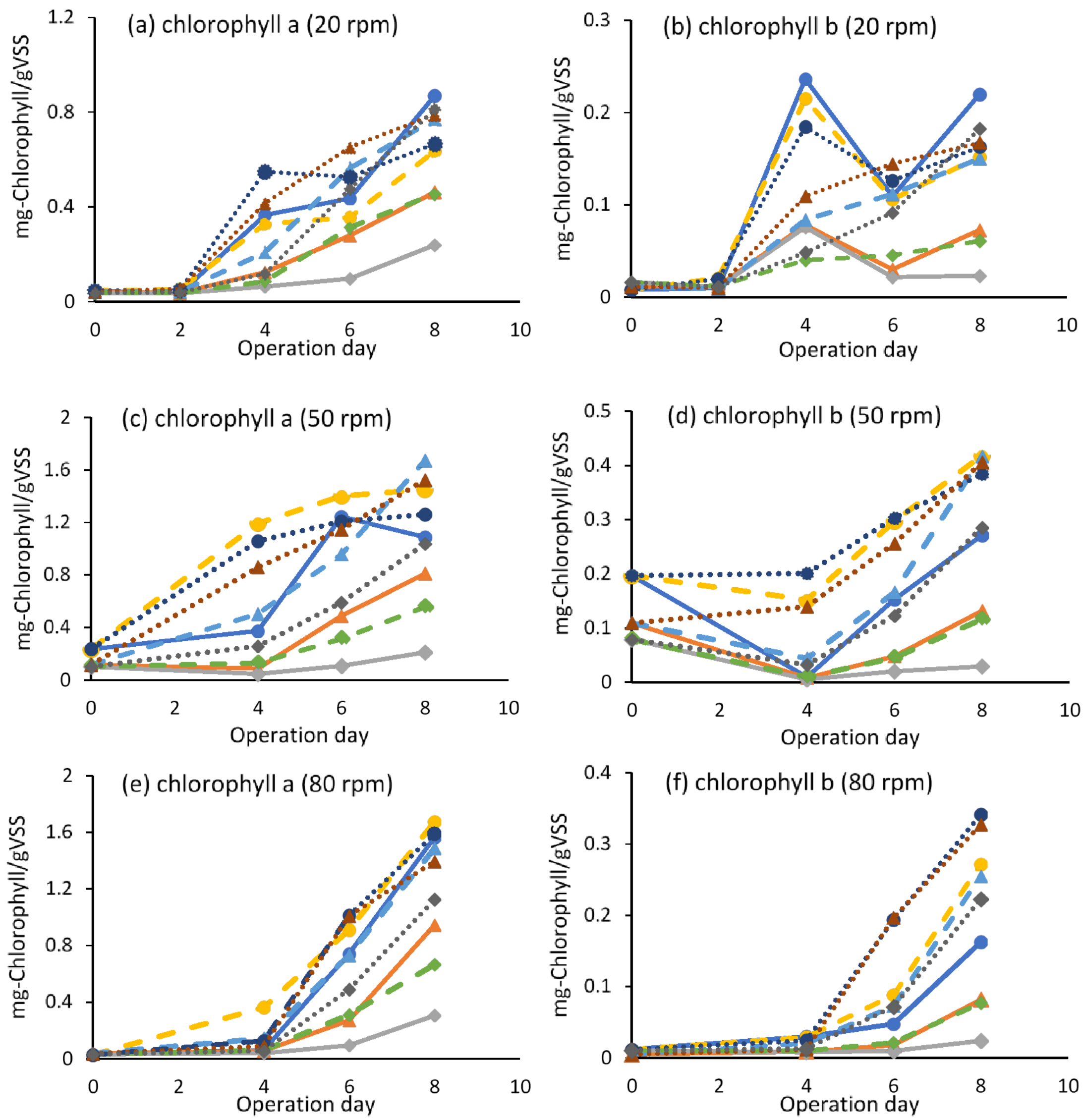

Figure 6. Changes of phototrophic pigments in batches. Chlorophyll *a* at (a) 20 rpm, (c) 50 rpm, and (e) 80 rpm. Chlorophyll *b* at (b) 20 rpm, (d) 50 rpm, and (f) 80 rpm. Different line styles represent different light conditions. Solid (—) lines: 6.4 KLux. Dashed (--) lines: 12.7 KLux. Dotted (……) lines: 25 KLux irradiances. The symbol (○) represents x4 dilution, (Δ) x2 dilution, and (◊) x1 dilution sets.

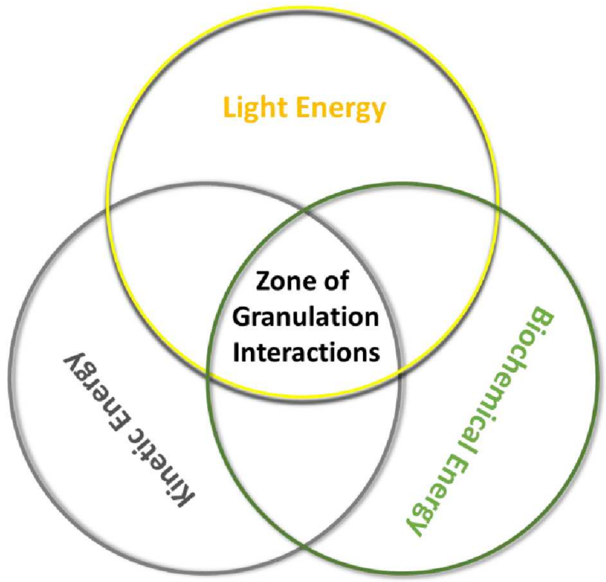

Figure 7. Energy interaction for OPG granulation. The zone of interaction presents potential conditions where the interaction of different abiotic stresses promote granular biotic responses.